Supporting Information

Phenyl-Incorporated Polyorganosilica Membranes with Enhanced Hydrothermal Stability for H_2/CO_2 Separation

Vinh Bui[1], Varun R. Satti[1], Elizabeth Haddad[1], Ameya Manoj Tandel[1], Narjes Esmaeili[1], Sai Srikar Chundury[1], Fathy Attia[1], Lingxiang Zhu[2,3], and Haiqing Lin*[1]

[1] Department of Chemical and Biological Engineering, University at Buffalo, The State University of New York, Buffalo, NY 14260, United States
[2] U.S. Department of Energy, National Energy Technology Laboratory, Pittsburgh, PA 15236, United States
[3] NETL Support Contractor, 626 Cochrans Mill Road, P.O. Box 10940, Pittsburgh, PA 15236, United States

* Corresponding author: Haiqing Lin, E-mail: haiqingl@buffalo.edu

1. Supplementary figures

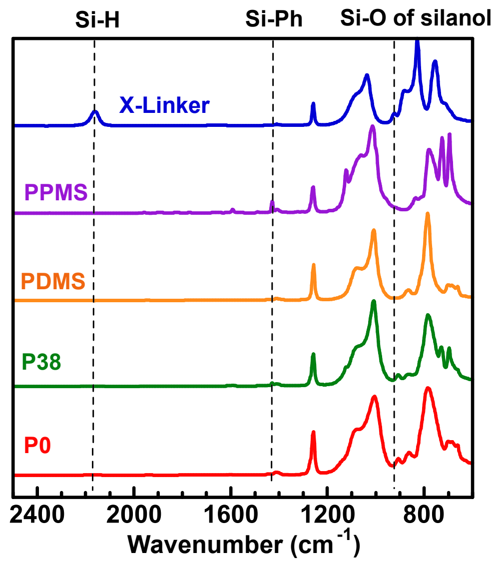

Fig. S1. FTIR spectra of polymer precursors and the assigned peaks: Si-H (2165 cm^{-1}), Si-Ph (1430 cm^{-1}), and Si-O stretching in Si-OH (907 cm^{-1}). The disappearance of Si-H in P0 and P38 confirms a successful hydrosilylation reaction, and the appearance of Si-O in Si-OH suggests the hydrolysis and oxidation reaction of the Si-H group.[1]

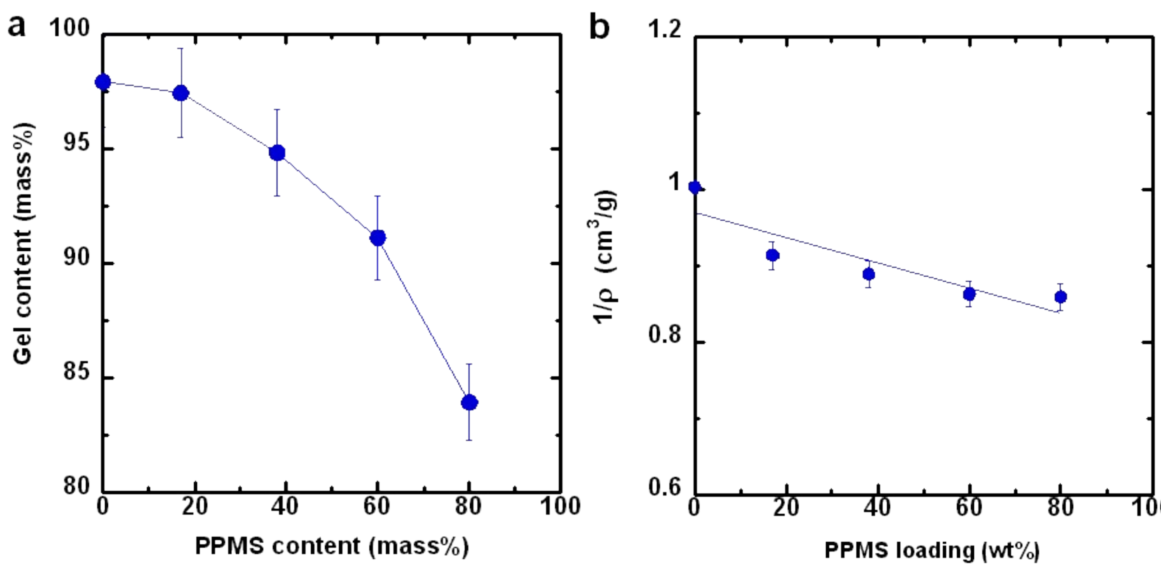

Fig. S2. Characterization of Pxx freestanding films as a function of the PPMS loading, including (a) gel content and (b) density.

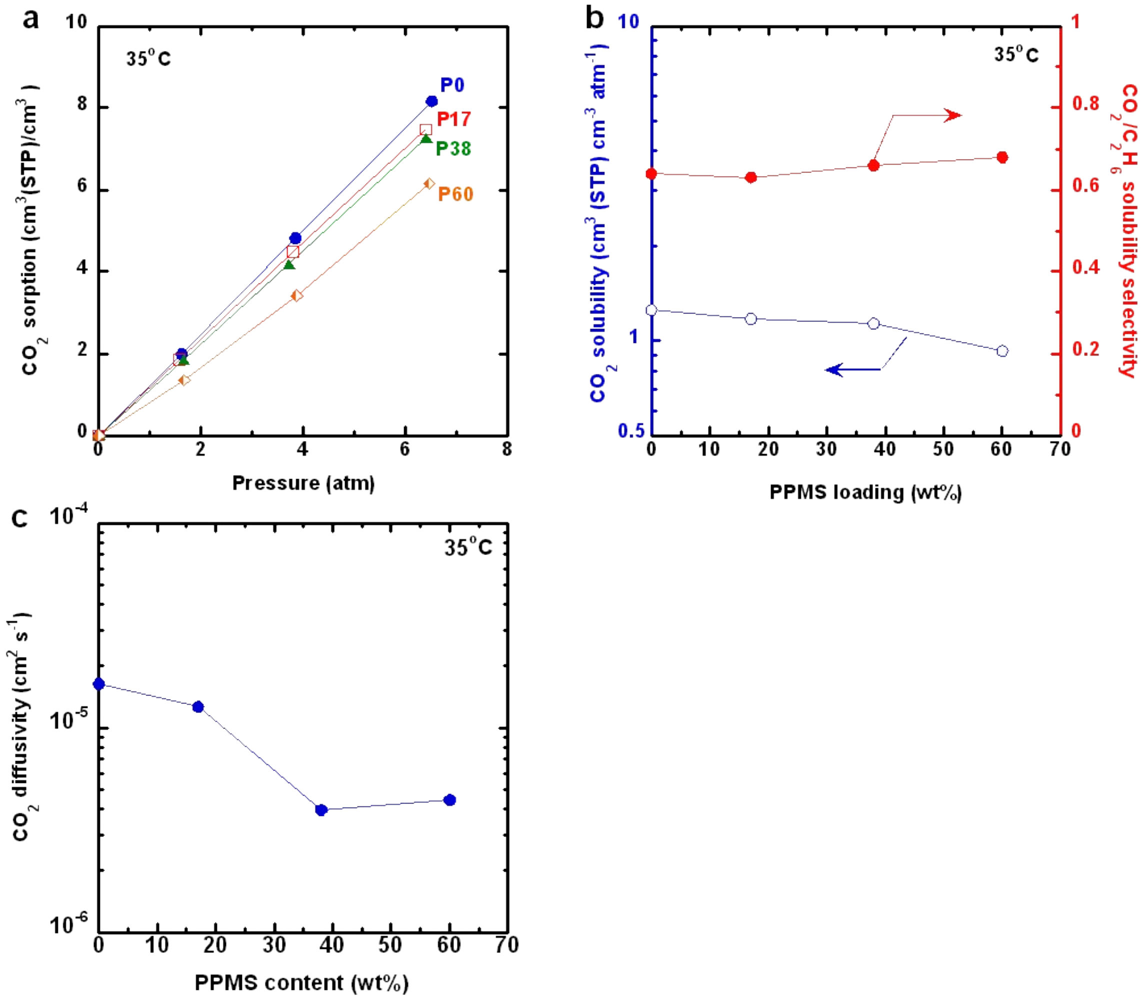

Fig. S3. Sorption and diffusion in Pxx films at 35 °C. (a) CO_2 sorption isotherms, (b) CO_2 solubility and CO_2/C_2H_6 solubility selectivity, and (c) CO_2 diffusivity. H_2 and N_2 sorption is below our detection limit, and therefore, non-polar C_2H_6 is used as a marker.

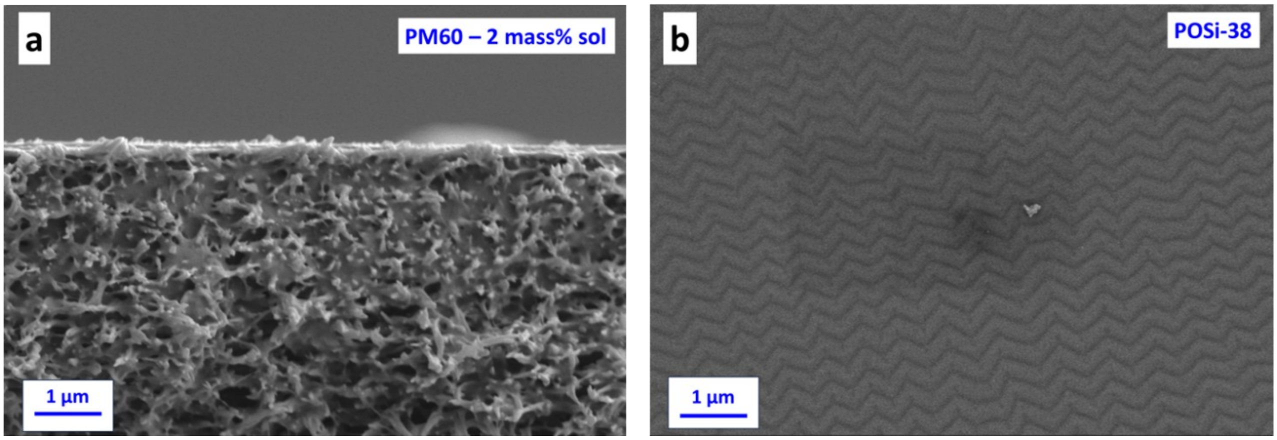

Fig. S4. (a) Cross-section SEM image of PM60 membrane prepared at 2 mass% solution, where severe pore penetration of polysilxoane leads to non-uniform coating of polysilxoane layer, and thus unsuitable for POSi membrane fabrication. (b) Surface SEM of POSi38.

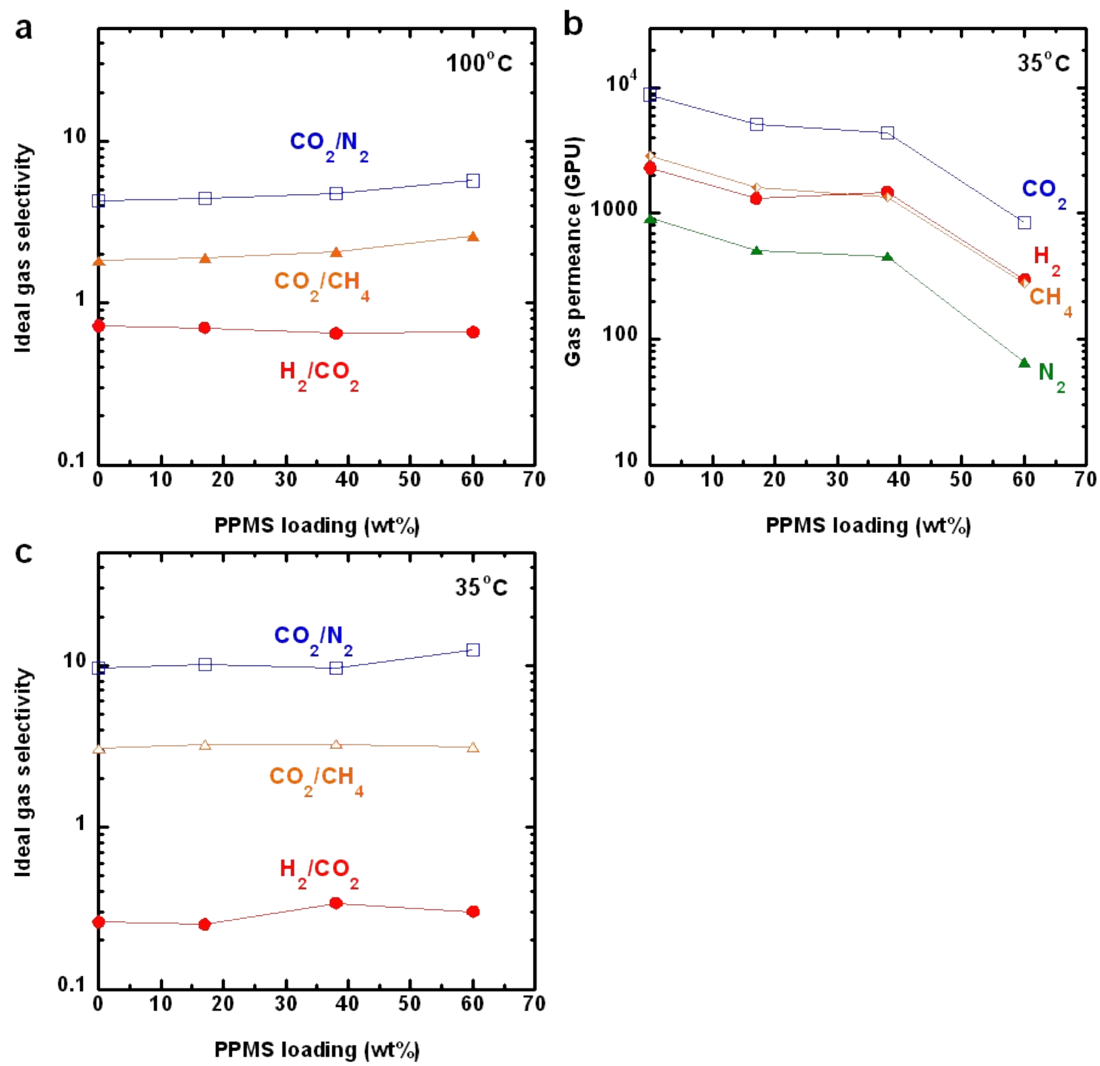

Fig. S5. Pure-gas transport properties of PMxx membranes. (a) Gas selectivity at 100 °C. (b) Gas permeance and (c) selectivity at 35 °C.

2. Supplementary tables

Table S1. Hydrothermal stability of representative silica membranes for gas separations. TEOS: tetraethyl orthosilicate; BTESE: 1,2-bis(triethoxysilyl)ethane; BTESP: bis(triethoxysilyl)propane; DMDPS: dimethoxydiphenylsilane; and MTES: methyltriethoxysilane.

Silica membranes	Fabric-ation	Hydrothermal conditions			Test temp. (°C)	Separation (A/B)	Before HT		After HT	
		Water vapor (kPa)	Temp (°C)	Duration (h)			Gas A permeance (GPU)	A/B selectivity	Gas A permeance (GPU)	A/B selectivity
TEOS[2]	CVD	16.5	600	130	600	H_2/CO_2	1450	1500	160	520
DMDPS[3]	CVD	3.4	300	226	300	H_2/N_2	2100	~900	2100	~1000
Al-doped TEOS[2]	CVD	16.5	600	130	600	H_2/CO_2	590	400	447	70
BTESE[4]	Sol-gel	101	100	72	200	H_2/CO_2	1340	~3	1200	~3
Zr-doped BTESE[4]	Sol-gel	101	100	72	200	H_2/CO_2	540	12	~300	12
Nb-doped BTESE[5]	Sol-gel	150	200	300	200	H_2/CO_2	205	115	92	206
F-doped BTESP[6]	Sol-gel	50	300	7	200	He/CF_4	1200	100	1500	100

Table S2. Prepolymer composition, glass transition temperature, and gas transport properties at 35 °C and 60 psig for Pxx films.

Pxx	Prepolymer composition (mass%)			Phenyl (mass%)	T_g (°C)	Gas permeability (Barrer)				Selectivity		
	*v*PDMS	*v*PPMS	PMHS			H_2	CO_2	N_2	CH_4	CO_2/N_2	CO_2/CH_4	H_2/CO_2
P0	77	0	23	0	< -90	770	2700	290	890	9.3	3.3	0.28
P17	63	17	21	9.5	-60	550	2200	200	670	11	3.3	0.25
P38	45	38	17	22	-28	400	2000	150	430	13	4.5	0.21
P60	26	60	13	34	-26	150	590	41	120	14	4.9	0.25
P80	11	80	9	45	-25	82	300	18	32	17	9.4	0.25

Table S3. Surface morphology of PMxx and POSixx membranes. The estimated area increase is calculated by dividing the arclength of the wave structure over the straight length that covers the wave structure. The arclength is determined using ImageJ analysis.

Membranes	Thickness (nm)		Wavelength (nm)	Amplitude (nm)	Surface area increase
	F-20	SEM			
PM0	340 ± 60	260 ± 20	-	-	-
PM17	390 ± 70	330 ± 70	-	-	-
PM38	330 ± 70	400 ± 20	-	-	-
PM60	990 ± 60	950 ± 50	-	-	-
POSi-0	-	340 ± 30	340 ± 20	23 ± 4	4%
POSi-17	-	370 ± 40	430 ± 10	36 ± 8	7%
POSi-38	-	360 ± 30	450 ± 30	35 ± 3	6%
POSi-60	-	990 ± 40	230 ± 20	30 ± 5	15%

Table S4. Surface atomic ratio of Pxx, POSixx, and HT-POSixx.

Samples	Atomic composition (mol%)			Atomic molar ratio		
	C	O	Si	O/Si	C/O	C/Si
Polysiloxanes						
P0	49.8 ± 1.3	27.2±0.7	22.9±0.7	1.19±0.05	1.83±0.07	2.18±0.09
P17	52.4 ± 1.2	25.7±0.6	21.9±0.6	1.18±0.04	2.04±0.07	2.40±0.08
P38	54.0 ± 0.9	24.9±0.4	21.1±0.1	1.18±0.04	2.17±0.05	2.56±0.08
P60	55.4 ± 0.6	24.2±0.4	20.4±0.2	1.18±0.02	2.29±0.04	2.71±0.03
Polyorganosilica (POSi)						
POSi0	21.7±0.6	51.9±0.76	26.4±0.2	1.97±0.03	0.42±0.01	0.82±0.02
POSi38	29.8±1.9	45.6±1.81	24.6±0.1	1.86±0.07	0.66±0.05	1.21±0.08
POSi60	26.0±1.1	49.5±0.91	24.5±0.3	2.0±0.1	0.52±0.02	1.06±0.05
HT-POSi						
HT-POSi0	28.3±0.6	45.3±0.8	26.4±0.4	1.72±0.04	0.63±0.02	1.07±0.03
HT-POSi38	31.3±1.0	44.1 ±1.0	24.6±0.2	1.79±0.04	0.71±0.03	1.27±0.04
HT-POSi60	29.5±1.2	45.8±1.1	24.7±0.1	1.85±0.05	0.64±0.03	1.19±0.05

Table S5. XPS peak deconvolution of Pxx, POSixx, and HT-POSixx.

Samples	C 1s deconvolution (%)		Si 2p deconvolution (%)		
	C-H or C-C (284.6 eV)	C-O (286 eV)	Si-$(O)_2$ (102.1 eV)	Si-$(O)_3$ (102.8 eV)	Si-$(O)_4$ (103.4 eV)
Pristine polysiloxanes					
P0	100	0	70	30	0
P17	100	0	70	30	0
P38	100	0	77	23	0
P60	100	0	71	29	0
Polyorganosilica (POSi)					
POSi0	87	13	12	15	73
POSi38	85	15	20	24	56
POSi60	87	13	18	16	66
HT-POSi					
HT-POSi0	81	19	15	25	60
HT-POSi38	81	19	20	18	62
HT-POSi60	85	15	15	17	68

Table S6. Gas permeance of the PMxx membranes and the ratio of the estimated gas permeability to the measured values for the corresponding Pxx films at 35 °C.

Membranes	F20 Thickness (nm)	Gas permeance (GPU)				Permeability ratio			
		H_2	CO_2	N_2	CH_4	H_2	CO_2	N_2	CH_4
PM0	340 ± 60	2300	8800	920	2900	1.0	1.1	1.1	1.1
PM17	390 ± 70	1300	5200	510	1600	0.92	0.92	1.0	0.93
PM38	330 ± 70	1500	4400	460	1350	1.2	0.72	1.0	1.0
PM60	990 ± 60	310	870	70	280	2.0	1.4	1.7	2.3

Table S7. Effect of the feed pressure on pure-gas transport properties of POSi membranes at 100 °C.

Membranes	Feed pressure (psig)	Gas permeance (GPU)				Selectivity	
		H_2	CO_2	N_2	CH_4	H_2/CO_2	H_2/CH_4
POSi0	20	140	2.3	0.28	0.45	61	311
	40	140	2.4	0.29	0.46	58	304
	60	140	2.5	0.29	0.41	56	341
POSi17	20	160	2.5	0.76	1.2	64	133
	40	160	2.7	0.81	1.1	59	145
	60	160	2.9	0.86	1.0	55	160
POSi38	20	130	3.1	1.4	1.6	42	81
	40	140	3.5	1.4	1.5	40	93
	60	140	3.5	1.4	1.5	40	93
POSi60	40	120	5.7	1.3	1.6	21	75
	60	120	5.8	1.3	1.5	21	80

Table S8. Calculated gas permeance through different regions of POSi membranes using resistance in a parallel and series model.

Membranes	Gases	Q_A (GPU)	Silica layer			Polysiloxane layer	
			$Q_{A,Si}$ (GPU)	$Q_{A,dSi}$ (GPU)	$Q_{A,kSi}$ (GPU)	$Q_{A,PM}$ (GPU)	Resistance portion (%)
POSi0	H_2	140	151	150	1.2	3300	4.2
	CO_2	2.5	2.4	2.2	0.25	4600	0.05
	N_2	0.30	0.31	~ 0	0.31	1100	0.03
	CH_4	0.41	0.41	0	0.41	2500	0.02
POSi17	H_2	160	183	180	2.8	1600	10
	CO_2	2.9	2.9	2.3	0.60	2300	0.13
	N_2	0.86	0.86	0.10	0.76	530	0.16
	CH_4	1.0	1.0	0	1.0	1200	0.08
POSi38	H_2	140	174	170	4.3	950	15
	CO_2	3.5	3.5	2.6	0.91	1500	0.23
	N_2	1.4	1.4	0.28	1.1	310	0.45
	CH_4	1.5	1.5	0	1.5	710	0.21
POSi60	H_2	120	194	190	4.3	320	38
	CO_2	5.8	5.9	5.0	0.91	490	1.2
	N_2	1.3	1.3	0.21	1.1	86	1.5
	CH_4	1.5	1.5	0	1.5	190	0.79

Table S9. H_2/CO_2 separation performance of POSi before and after vapor treatment at 100 °C.

Membranes	Before vapor treatment		After vapor treatment	
	H_2 permeance (GPU)	H_2/CO_2 selectivity	H_2 permeance (GPU)	H_2/CO_2 selectivity
POSi0	143	57	160	16
POSi17	159	59	150	8.5
POSi38	144	41	98	19
POSi60	130	13	110	11

References

1. K. Efimenko, W. E. Wallace and J. Genzer, *J. Colloid Interface Sci.*, 2002, **254**, 306-315.
2. Y. Gu, P. Hacarlioglu and S. T. Oyama, *J. Membr. Sci*, 2008, **310**, 28-37.
3. Y. Ohta, K. Akamatsu, T. Sugawara, A. Nakao, A. Miyoshi and S.-I. Nakao, *J. Membr. Sci*, 2008, **315**, 93-99.
4. M. ten Hove, M. W. J. Luiten-Olieman, C. Huiskes, A. Nijmeijer and L. Winnubst, *Sep. Purif. Technol.*, 2017, **189**, 48-53.
5. H. Qi, H. Chen, L. Li, G. Zhu and N. Xu, *J. Membr. Sci*, 2012, **421-422**, 190-200.
6. I. Rana, H. Nagasawa, K. Yamamoto, T. Gunji, T. Tsuru and M. Kanezashi, *J. Membr. Sci*, 2022, **644**, 120083.